




## Suspended solid removal efficiency of plate settlers and tube settlers analysed by CFD modelling

W. M. L. K. Abeyratne<sup>a</sup>, S. B. Weerakoon <sup>a</sup>, Panduka Neluwala <sup>a,\*</sup> and Harsha Ratnaweera <sup>b</sup>

<sup>a</sup> Department of Civil Engineering, University of Peradeniya, Peradeniya 20480, Sri Lanka

<sup>b</sup> Norwegian University of Life Sciences, Universitetstunet 3, P.O. Box 5003, Ås NO-1432, Norway

\*Corresponding author. E-mail: pandukaneluwala@eng.pdn.ac.lk

 SBW, 0000-0002-3671-6241; PN, 0000-0002-1686-3412; HR, 0000-0003-1456-2541

### ABSTRACT

Removal of suspended solids from raw water is an essential process in water treatment plants. Conventional sedimentation tanks in water treatment plants occupy a large area and become expensive in urban areas. The use of plate settlers or tube settlers in sedimentation tanks to increase the efficiency and hence reduce the footprint of sedimentation tanks is an economical solution in water treatment. This study investigated the effectiveness of plate and tube settlers compared to conventional settlers in a water treatment plant. A three-dimensional Computational Fluid Dynamics (CFD) model was set up using ANSYS-CFX 17.2. Seven cases (a conventional settler, three plate settlers and three tube settlers) were analysed to compare the settler performances. The maximum removal efficiencies of all solid classes were approximately equal in plate and tube settlers with the same plate spacing and tube depth: around 100%, 67%, 28% and 9% for the solid classes with particle diameters of 41, 17, 9.5 and 5.0  $\mu\text{m}$ , respectively. The settling efficiency remained unchanged with the increase of the plate settling area beyond 60% of the conventional settler area under the given tank and flow conditions. The tube cross-section shape does not affect the particle removal efficiency of a tube settler.

**Key words:** computational fluid dynamics, plate settlers, sedimentation tanks, suspended solids, tube settlers

### HIGHLIGHTS

- Plate settlers and tube settlers are increasingly used to reduce the water treatment plant footprint with the increasing land prices in urban areas.
- The present study compares the efficiency of these settlers in the removal of suspended solids of different size classes by three-dimensional computational modelling using ANSYS CFX.
- The model developed here can be used to upgrade existing conventional settling tanks paying due attention to the removal efficiency of different solid classes.

## GRAPHICAL ABSTRACT

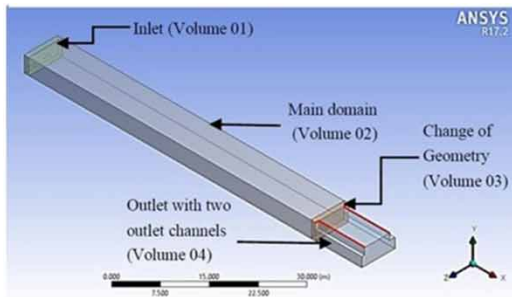
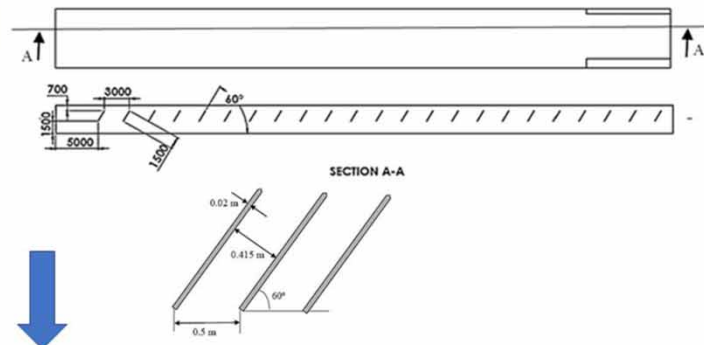
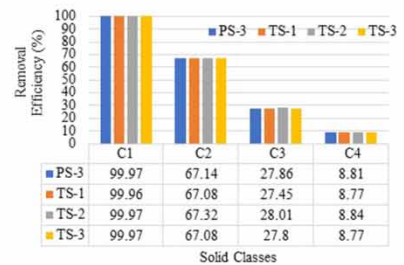
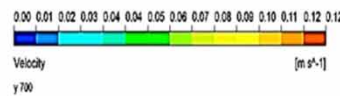


## Plate Settlers and Tube Settlers Analysed by CFD Modelling



(a)



## 1. INTRODUCTION

The sedimentation process where suspended solids (SS) are removed from raw water by either chemical or biological processes is one of the essential processes in water treatment plants. The conventional sedimentation process relies on the net downward force due to the difference in density between particles and fluid (Carlsson 1998). The water treatment plants are generally located in urban areas, and the large area occupied by the conventional sedimentation tanks tends to be responsible for up to 30% of the total construction cost of a water treatment plant (Tamayol *et al.* 2008). Many factors affect the capacity and performance of sedimentation tanks: solids characteristics, fluid characteristics, and design parameters such as tank type, solid loading rate, surface loading rate, hydraulic retention time, weir placement, and solid removal mechanism (Asgharzadeh *et al.* 2011).

Several efforts have been made by designers to reduce the costs associated with the sedimentation tanks; the conventional settlers are modified by inclined plates or tubes to reduce the particle settling depth and thereby to reduce the detention time and the volume of the settling basins. A plate settler is a sedimentation tank with multiple inclined plates placed parallel to each other, which combine to form a large effective settling area. However, the tube settler has a group of pipes or channels with small cross-sectional area contiguous with each other. These are usually made of lightweight materials (PVC or similar material), with or without a supporting frame. These tubes can be of different shapes including square, circular and hexagonal (Fadel 1985; Gurjar *et al.* 2017).

The use of tube settlers and plate settlers is the result of economical technological development which helps to increase design surface loads in sedimentation tanks. They increase the capacity of sedimentation tanks and drastically reduce the plant footprint due to the significantly reduced particle settling path and settling time by increasing the effective settling area (Faraji *et al.* 2013; Al-kizwini 2015; Balwan *et al.* 2016; Fouad *et al.* 2016; Al-Dulaimi & Racoviteanu 2018; Bhatia 2018). The superior performance of tube settlers and plate settlers compared to conventional sedimentation tanks is well documented. Computational fluid dynamics (CFD) tools have been applied to optimize the design of contact chambers and conventional sedimentation tanks to minimize short-circuiting and inactive volumes. The determination of the effect of inclination angle, length, and diameter of the tubes on the SS removal efficiency has been the subject of many experimental and numerical studies (Faraji *et al.* 2013; Tarpagkou & Pantokratoras 2014; Balwan *et al.* 2016; Al-Dulaimi & Racoviteanu 2018, Sharma & Bhatia 2018, Nguyen *et al.* 2019a).

Although experimental investigations have compared the performances of tube settlers and plate settlers, their performances have not been systematically evaluated and compared in detail under sediment parameters of raw water such as the particle size distribution of SS. Also, the effect of different cross-sectional shapes of the tubes has not been documented in the previous studies.

The detailed analysis referred to SS of different sizes is essential to understand removal efficiency of different sediment classes with varying sizes of particles in various designs. The application of CFD to simulate the settling process has been widely accepted due to its visualization capabilities and data on the hydraulic regime under different conditions of geometry and flow pattern, density and vortex zone, mass fraction, and settling velocity of particles (Nguyen *et al.* 2019a).

The objectives of this study are to evaluate the efficiency of tube settlers with tubes of different cross-sectional shapes in use, for removing turbidity and to compare the efficiencies of conventional settlers, plate settlers, and tube settlers for removing turbidity of water within the sedimentation tanks of water treatment plants. In this study, a CFD model setup using ANSYS-CFX 17.2 solves the bulk momentum and continuity equations for the mixture of solids and fluid using the Algebraic Slip Model (ANSYS 2016). The flow field, SS concentration field, and suspended solids removal efficiency ( $R\%$ ) in conventional settlers, plate settlers, and tube settlers are calculated and compared.

## 2. MATERIALS AND METHODS

### 2.1. Computational model

The three-dimensional model of sedimentation tanks was set up using the commercial CFD software ANSYS CFX 17.2, which has been extensively used in modelling of complex flows (Tarpagkou & Pantokratoras 2014, Yu *et al.* 2016; Nguyen *et al.* 2019b). Flow in the sedimentation tank was defined as a liquid–solid multiphase dispersed flow where sediment particles (dispersed phase component) are mixed with water (continuous phase component) forming a continuous medium mixture with a varying composition and density. This mixture density is affected by the presence of solids in different locations.

Eulerian multi-phase mixture model in which all the phases are considered as continuous was used for the simulations because the overall motion of the particle is of interest rather than tracking individual particles. The mixture model used in ANSYS CFX is the ‘Algebraic Slip Model’ (ASM), which is a simplified version of Ishii (1975). The ASM adopts one fluid with a variable composition where continuous medium with dispersed phase components of different diameters and densities is used.

The three-dimensional flow field is governed by bulk continuity Equation (1) and bulk momentum Equation (2), which are obtained by summing the corresponding equations of all phases in the mixture (ANSYS 2016):

$$\frac{\partial \rho_m}{\partial t} + \frac{\partial (\rho_m U_m^i)}{\partial x_i} = 0 \quad (1)$$

$$\frac{\partial \rho_m U_m^i}{\partial t} + \frac{\partial \rho_m U_m^j U_m^i}{\partial x^j} = -\frac{\partial P}{\partial x^i} + \frac{\partial (\tau_m^{ij} + \tau_{Tm}^{ij} + \tau_{Dm}^{ij})}{\partial x^j} + g^i \rho_m \quad (2)$$

where  $x^i$  is the Cartesian coordinate in the  $i$  direction,  $U_m^i$  is the mixture flow velocity in the  $i$  direction,  $P$  is the pressure,  $t$  is time,  $g^i$  is the acceleration of gravity,  $\tau_m^{ij}$  is viscous diffusion stress,  $\tau_{Tm}^{ij}$  is turbulent diffusion stress, and  $\tau_{Dm}^{ij}$  is apparent diffusion stress.

The concentration field for each class of solids in the tank is determined by the mass balance equation. For each class of mass fractions ( $Y_{s,n}$ ) after using Boussinesq approximation,

$$\frac{\partial (\rho_m Y_{s,n})}{\partial t} + \frac{\partial (\rho_m Y_{s,n} (U_m^j + U_{S_{s,n}}^j))}{\partial x^j} = \frac{\partial}{\partial x^j} \left( \mu_m \frac{\partial Y_{s,n}}{\partial x^j} + \frac{\mu_{tm}}{0.9} \frac{\partial Y_{s,n}}{\partial x^j} \right) \quad (3)$$

$$U_{S_{s,n}} = V_s = \frac{\rho_w g (S_{s,n} - 1) d_{s,n}^2}{18 \mu_w} \quad (4)$$

where  $U_S$  is the slip velocity of particles,  $\mu_t$  is the eddy viscosity,  $\mu$  is the dynamic viscosity, and  $Y$  is the mass fraction. The slip velocity  $U_S$  is the settling velocity of particles ( $V_s$ ) determined using Stokes’ law given in Equation (4) and applied to the settling of spherical particles in a laminar flow.  $\rho$  is the density,  $g$  is gravitational acceleration,  $S_s$  is the specific gravity of

solids, and  $d_{s,n}$  is the diameter of solids (Henricks 2011). The subscripts  $w$ ,  $m$  and  $s$ ,  $n$  denote quantities for water, mixture, and class of solids.

## 2.2. Model validation

The model was validated using data from the study on settling tanks of the water treatment plant of Acharnes and Athens in Greece by Stamou & Gkesouli (2015). Model validation was done for two scenarios S-1 and S-2 corresponding to inlet mass flow rates of 0.25 and 0.31 m<sup>3</sup>/s, respectively. The model performance was verified by comparing the streamline patterns, velocity contour plots of S-1, and suspended solid concentration and removal efficiency of S-2 with the observations presented by Stamou & Gkesouli (2015). The solid concentration was calculated using the volume fractions of solids.

### 2.2.1. Geometry

Acharnes water treatment plant uses 16 similar rectangular sedimentation tanks as shown in Figure 1(a). Each tank has a length of 73.2 m, a width of 14.4 m, and an average water depth of 3.5 m. Each tank has four inlet openings near the bottom of the tank through which the effluent of flocculation tanks enters the sedimentation tanks. The effluent exits through a series of V-notch weirs installed at three outlet channels. The flow rate varies from 0.25 to 0.31 m<sup>3</sup>/s. The plan view of a tank is given in Figure 1(b). Since the tank is symmetrical around the  $xy$  plane, only one half of the tank was modelled to reduce the computational time.

The geometry was developed in four volumes as Inlet, Outlet, Main Domain, and Change of Geometry to make the meshing more effective. The fluid domain was developed using the ANSYS design modeller (Figure 2).

### 2.2.2. Computational grid

The main domain and outlet volume shown in Figure 2 were meshed using structured grids with hexahedral elements. The regions of complex geometries including inlet and change of geometry shown in Figure 2 were meshed using unstructured grids. The refined mesh was used at the inlet openings and outlet channels to derive detail flow properties in these regions, which are of more interest in the study. The computational grids consisted of approximately 219,300 elements. To ensure that

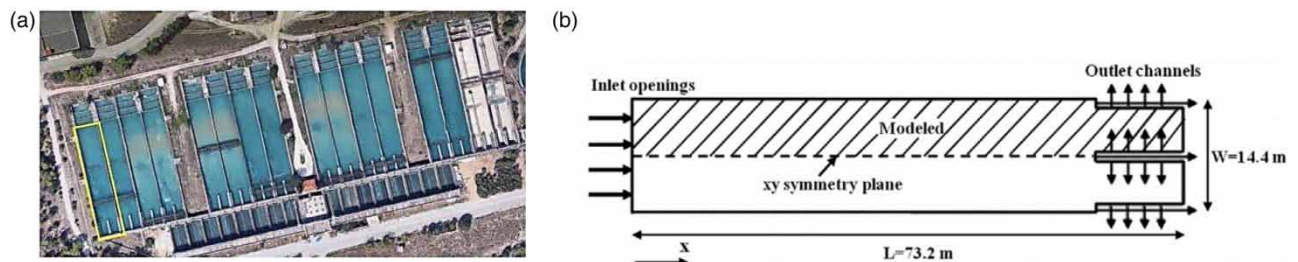


**Figure 1** | (a) Sixteen similar rectangular tanks in the Acharnes water treatment plant and (b) plan view of the rectangular tank (Stamou & Gkesouli 2015; Gkesouli 2018).

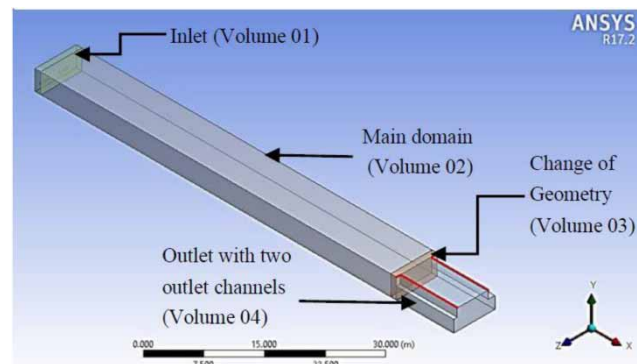


**Figure 2** | The tank geometry developed in the ANSYS Design modeller.

the results are grid independent, several preliminary computations were carried out before choosing this element size: the grid independency study results are shown in Table S1 in Supplementary Information.

### 2.2.3. Boundary definition

The computational domain, which is half of a sedimentation tank, is shown in Figure 3. At the two inlet openings, the parallel flow was applied with a uniform horizontal velocity. The turbulence intensity was set at 5%. Inlet flow characteristics under the two scenarios are given in Table 1. Similar to that given in the study by Stamou & Gkesouli (2015), the inlet solids with a density of  $2,730 \text{ kg/m}^3$  were divided into four classes as given in Table 2 and assumed to be uniformly distributed across the inlet. The sum of the inlet mass flow rates was set as the outlet boundary condition. The bottom of the tank was set as a no-slip smooth wall, and solids were assumed to be deposited and removed from the domain. The direct settling of large particles is expected on the bottom, and other particles are expected to settle and slip along the inclined plates. As noted in the modelling of sedimentation tanks by Gao (2019), the SS removal efficiency is not seriously affected by this no-slip smooth wall assumption to cause a change in the comparisons in the study. The top surface (free surface) of the domain was treated as a free-slip wall, and hence, the normal velocity component and normal gradients of other variables were set to zero. All the vertical walls except the right side of the domain at which symmetry condition was used were treated as hydraulically smooth walls, and no-slip condition was applied. The advection scheme used was upwind. The turbulence model used was the standard  $k-\omega$  model.

### 2.3. Model application

The validated model was applied to investigate the effect of (a) the number of plates on plate settler efficiency and (b) the tube cross-sectional shapes on the efficiency of tube settlers using the suspended solid removal efficiency ( $R\%$ ) in each case.  $R\%$  is determined using Equation (5), where  $S_{in}^i$  and  $S_{out}^i$  are the inlet and outlet solid concentrations, respectively, of the solid class  $i$  ( $i = 1-4$ ). The outlet-suspended solid concentrations are calculated using Equation (6), where  $VF_{solid}^i$  is the volume fraction of solids and  $\rho_{solid}$  is the density of solids.

$$R\% = \frac{\sum_{i=1}^4 S_{in}^i - \sum_{i=1}^4 S_{out}^i}{\sum_{i=1}^4 S_{in}^i} \times 100 \quad (5)$$

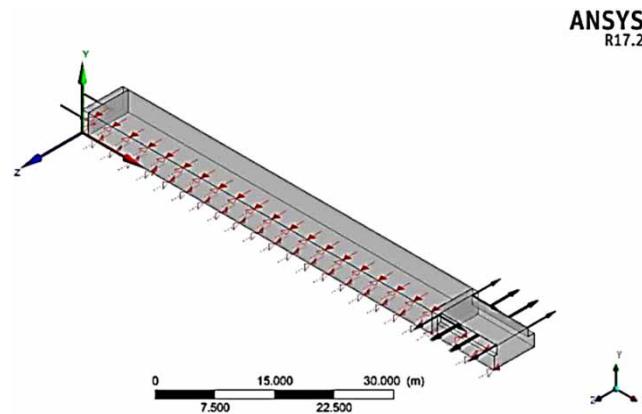


Figure 3 | Fluid domain with applied boundary conditions.

Table 1 | Inlet flow characteristics of the scenarios used for model verification

Scenario	Mass flow rate ( $\text{m}^3/\text{s}$ )	Inlet velocity (m/s)
S-1	0.25	0.119
S-2	0.31	0.149

**Table 2** | Details of the inlet suspended solid classes (Stamou & Gkesouli 2015)

Solid class	Solid diameter (μm)	Settling velocity (mm/s)	Scenario S-1		Scenario S-2	
			Inlet solid mass fraction MF <sub>in</sub>	Inlet solid concentration S <sub>in</sub> (mg/l)	Inlet solid mass fraction MF <sub>in</sub>	Inlet solid concentration S <sub>in</sub> (mg/l)
C1	41	1.6	0.45	3.15	0.45	3.15
C2	17	0.27	0.17	1.19	0.36	2.52
C3	9.5	0.086	0.23	1.61	0.04	0.28
C4	5	0.025	0.15	1.05	0.15	1.05
Total	1.00	7.00	1.000	7.00		

$$S_{out}^i = VF_{solid}^i \times \rho_{solid} \tag{6}$$

Seven cases were analysed for the evaluation of different settler performances. Those include (i) conventional settler, (ii) three different plate settlers with plate spacing of 3 m (PS-1) (Figure 4), 1 m (PS-2), and 0.5 m (PS-3) where spacing is measured streamwise (Figure 5), and (iii) three different tube settlers with rectangular (TS-1)-, hexagonal (TS-2)-, and hexagonal chevron (TS-3)-shaped tubes with an equal interior cross-sectional area of 2,170 cm<sup>2</sup>. The depth of the tubes (0.415 m) in the three tube settler configurations was equal to the plate spacing in the PS-3 (Figure 5). Hence, the particle settling depth and effective settling area of PS-3 and tube settler configurations were maintained approximately equal. Plates and tubes have been installed in the sedimentation tanks of Acharnes water treatment plant at an inclination of 60° to the horizontal plane. The wall thickness and length of tubes and plates were kept constant at 0.02 and 1.5 m, respectively. The percentage of the increased settling area α of the plate settlers was calculated using Equation (7). A<sub>0</sub> is the settling area of conventional settler, and A<sub>i</sub> is the projected area of plates calculated by Equation (8), where n is the number of plates, W is the width of a plate, and L is the length of a plate (Nguyen *et al.* (2019a)): the α values of PS-1, PS-2, and PS-3 were 24, 60, and

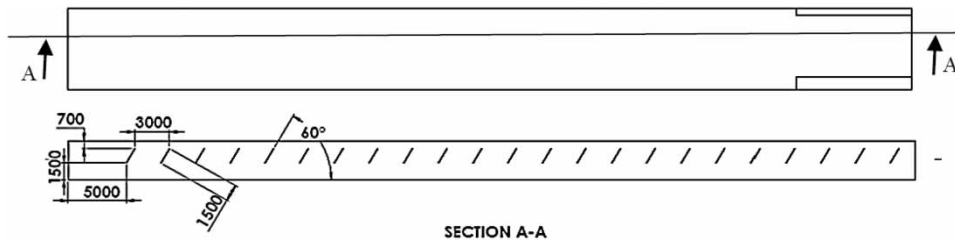


**Figure 4** | Longitudinal section of plate settler configuration of PS-1 (all dimensions are in millimetres).

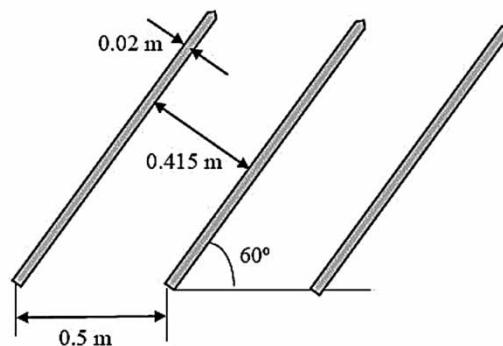


**Figure 5** | Plate arrangement in PS-3.

138%, respectively. The  $\alpha$  values of TS-1, TS-2, and TS-3 are approximately equal  $\alpha$  to PS-3. Simulations were carried out under the boundary conditions and SS characteristics of the scenario S-2.

$$\alpha = \frac{A_i}{A_0} \times 100\% \quad (7)$$

$$A_i = nWL \cos 60^\circ \quad (8)$$

### 3. RESULTS AND DISCUSSION

#### 3.1. Validation of the model

In the model validation, the streamline pattern in the  $xy$  plane (which is marked in Figure 2) at  $z = -1.9$  m and the velocity contour plot in the  $xz$  plane at  $y = 0.7$  m were compared for scenario S-1 – the comparisons are shown in Figures 6 and 7, respectively. The streamline pattern at  $z = -1.9$  m plane depicts an eddy (V1), which is formed due to the incoming jets from the inlet openings. This eddy is approximately 20 m in length (Stamou & Gkesouli 2015) as shown in Figure 6(a). V1 has been displayed to the same size satisfactorily in this study too (Figure 6(b)). Figure 7(a) and 7(b) similarly depict that the two jets entering through the inlet openings push the incoming water to the right side of the tank. The velocity inside the tank varies between 0 and 0.12 m/s and is in a similar pattern as shown in the two plots.

Stamou & Gkesouli (2015) report the turbidity measurements for the scenario S-2 at  $x = 63$  m at the plane 0.1 m away from the side wall of the tank. The suspended solid concentrations of the four solid classes were computed from the computed volume fractions at the same location for S-2, and the total SS concentrations are compared in Figure 8. Accordingly, the computed concentrations show a good agreement with the measured turbidity in the study by Stamou & Gkesouli (2015) with a correlation coefficient of 0.8. The volume fraction contour plots in the  $yz$  plane at  $x = 63$  m are shown in Figure S1, and the data used in Figure 8 are presented in Table S2 in Supplementary Information. The slight differences in the SS concentrations could be due to the assumptions made in the simplified ‘Algebraic Slip Model’ utilized in this study and also due to the possible errors in observations in this complex flow. The comparison of the percentage removal of solids classes is shown in Table 3. The removal efficiency of the solid class C1, which is the class of particles with the highest diameter, is 99% in the study by Stamou & Gkesouli (2015), while it is 100% in this study. The removal efficiency of the solid class

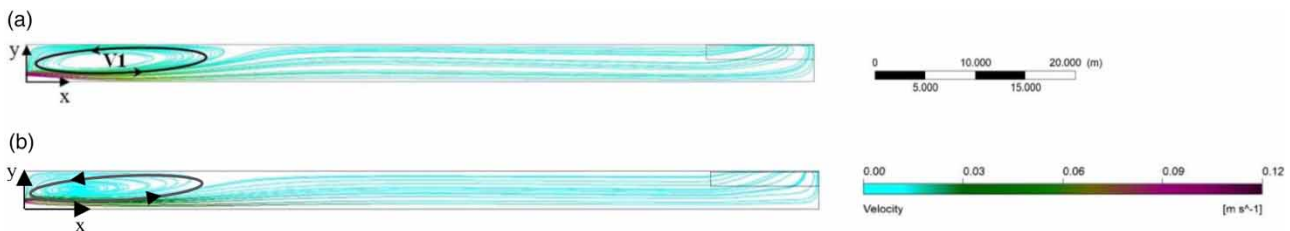


**Figure 6** | Streamline pattern in the  $xy$  plane at  $z = -1.9$  m: (a) Stamou & Gkesouli (2015) and (b) computed in this study.



**Figure 7** | Velocity contour plot in the  $xz$  plane at  $y = 0.7$  m: (a) Stamou & Gkesouli (2015) and (b) computed in this study.

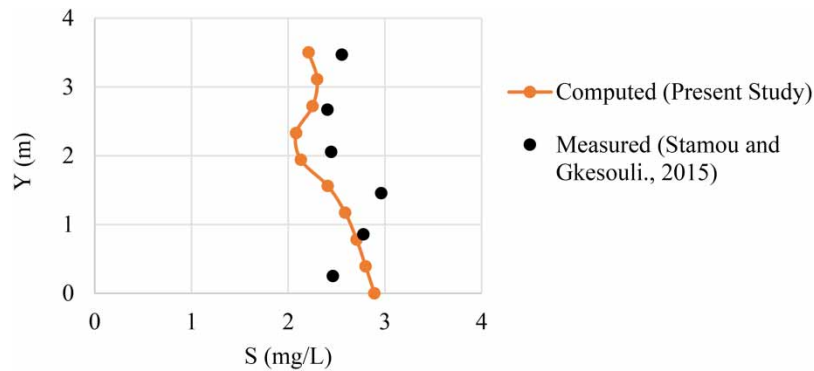


**Figure 8** | Variation of SS concentrations at  $x = 63$  m along the tank depth ( $y$ ) for the scenario S-2.

**Table 3** | Comparison of solids removal efficiencies

Solid class	Measured removal efficiency (Stamou & Gkesouli 2015)	Removal efficiency (computed in this study)
C1	99%	100%
C2	57%	55%
C3	25%	21%
C4	9%	8%

C4, which is the class of particles with the smallest particle diameter, is approximately 9% in the study by Stamou & Gkesouli (2015) and 8% in this study. The computed removal efficiencies of solid class C2 and solid class C3 show differences of 2 and 4%, respectively, with the measurements given in the study by Stamou & Gkesouli (2015). However, the total solid removal efficiencies  $R\%$  of the tank in scenario S-2 in the study by Stamou & Gkesouli (2015) and in this study show the same value of 67%.

### 3.2. Performance of plate settlers and tube settlers compared to that of conventional settler

Computed streamline patterns in the plate settlers and tube settlers under same boundary conditions given by Stamou & Gkesouli (2015) show a reduction in the size of the flow recirculation zone at the inlet region of the tank and an increased upward flow in the tank. The upward flows in plate and tube settlers provide a conducive flow pattern for particle settling compared to that of the conventional settling tank. Figure 9 shows the comparison of streamlines among the conventional settler, plate settler PS-1, and the tube settler TS-1. The particle removal efficiency ( $R\%$ ) increases as the number of plates is increased in the plate settlers (Figure 10). This can be attributed to the increasing effective settling area as well as the upward motions, and the reduction of the settling path of particles. However,  $R\%$  remained unchanged with the increase of the settling area beyond 60% of the conventional settler area for the given geometric and flow conditions. The reason for the limit of this removal efficiency could be the transport potential by the velocity head (kinetic energy) of the fluid, which depends on the head difference across the inlet and outlet and the head loss of the flow through the tank. However, this fact has to be investigated under different flow and geometric conditions.

In tube settler, it was found that the cross-section shape does not affect the removal efficiency as long as the tubes' cross-sectional area, length, and number of tubes are the same (Figure 11). Although the settling area has a significant effect on the SS removal efficiency, it is also important to investigate how the location of the tube/plate settlers and the ratio of height of the tubes/plates to the tank depth affect the SS removal efficiency.

These CFD simulations in plate settlers and tube settlers have given different removal efficiencies ( $R\%$ ) with respect to different particle diameters, which might be extremely difficult, if not impossible, to characterize by experimental studies. The maximum  $R\%$  values of different solid classes in different settlers are compared in Figures 12 and 13. According to Figure 13, the maximum  $R\%$  values of all solid classes in PS-3 are approximately equal to that of TS-1, TS-2, and TS-3. This is due to the equal spacing between plates of PS-3 (which is 0.415 m) and the depth of the tubes in the three tube settlers.



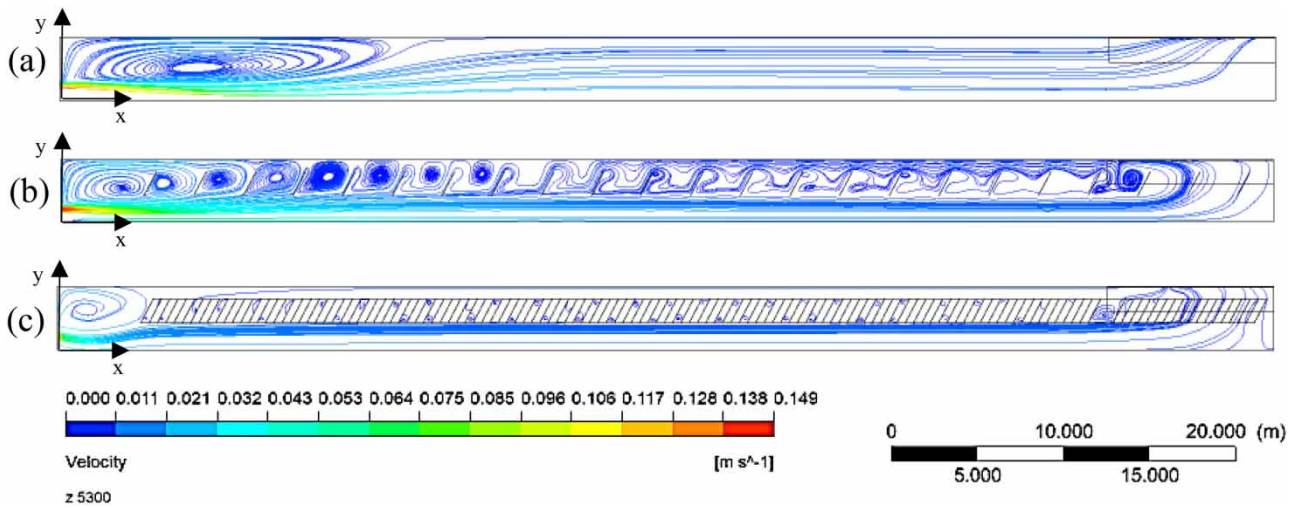


**Figure 9** | Comparison of streamline patterns at the plane  $z = -1.9$  m: (a) conventional settler, (b) PS-1, and (c) TS-1.

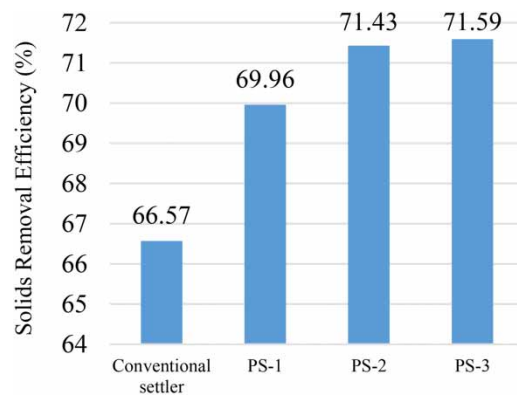


**Figure 10** | SS removal efficiency of plate settlers compared with conventional settler.

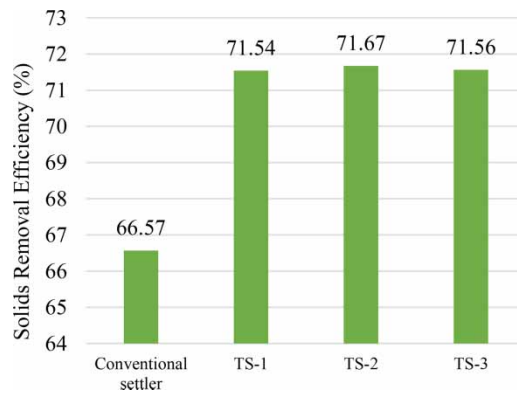


**Figure 11** | SS removal efficiency of tube settlers compared with conventional settler.

Therefore, the removal efficiency of particles of any size is mostly affected by the effective settling area and the particle settling depth. The maximum  $R\%$  values are around 100, 67, 28, and 9% for the solid classes with particle diameters 41, 17, 9.5, and  $5.0 \mu\text{m}$ , respectively. The maximum improvements of solid removal efficiencies were approximately 1, 10, and

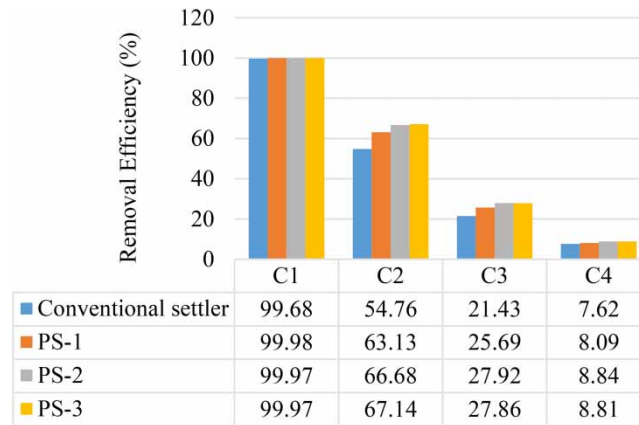


**Figure 12** | Comparison of removal efficiencies of conventional settler and plate settlers.

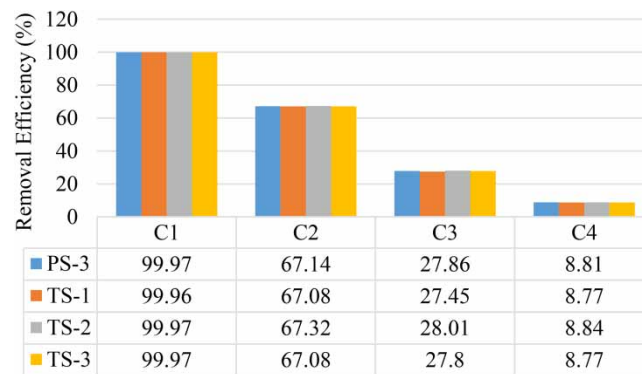


**Figure 13** | Comparison of removal efficiencies of plate settler and tube settlers.

3% for particles with a diameter of 41, 17, and 9.5  $\mu\text{m}$ , respectively, in both plate settler and tube settler, compared to the conventional settler.

Under the studied case, there is no significant difference in the performance of the three different types of settlers for the largest particle size. However, there is an indication of better performance of the plate settlers and tube settlers in removing smaller solid particles. This performance of different types of settlers could be significantly affected by flow fluctuations in settling tanks. This study shows that the CFD model developed can be applied for such detailed comparative studies. No doubt that such studies demand high-end computers.

The CFD modelling can be used to compare design changes in plate and tube settlers to predict and optimize the SS removal efficiency. In process modifications of full-scale units, CFD analysis could be used to avoid possible costly design errors. Furthermore, CFD analysis can also be a useful tool in the design modifications where the capacity increase is required without compromising the SS removal efficiency in a region with land area constraints.

#### 4. CONCLUSIONS

(1) Installing inclined plates and tubes in the conventional settling tank facilitated an increase in settling particles by reducing the recirculating zones and increasing the upward flow.

The solids removal efficiency of conventional settler increased by the installation of plates and tubes to attain low particle settling depth and high effective settling area.

The tube settler cross-sectional shape does not affect the removal efficiency as long as the tubes' cross-sectional area, length, depth, and number of tubes are kept constant.

- (2) Under the given tank and flow conditions in the studied case,
- the removal efficiency of plate settlers remained unchanged with the increase of the settling area beyond 60% of conventional settler settling area,
  - the maximum attainable removal efficiencies of all solid classes were approximately equal in plate settler PS-3 and tube settlers, and they were approximately 100, 67, 28, and 9% for solids with diameters of 41, 17, 9.5, and 5  $\mu\text{m}$ , respectively, and
  - there is no significant difference in the performance of the three different types of settlers with respect to smaller diameter particles, although the removal efficiency was enhanced by plates and tubes. The smallest diameter particle group <5  $\mu\text{m}$  still remained at almost 100% inside the tank, which limited the maximum attainable overall efficiency to 85%.

## ACKNOWLEDGEMENTS

The authors wish to extend their sincere gratitude to NORAD-NORHED Project 'LKA-13/0013-WaSo-Asia Project' for providing financial assistance for conducting this research study.

## DATA AVAILABILITY STATEMENT

All relevant data are included in the paper or its Supplementary Information.

## CONFLICT OF INTEREST

The authors declare there is no conflict.

## REFERENCES

- Al-Dulaimi, S. M. S. & Racoviteanu, G. 2018 *Performance of the tube settle clarification at different inclination angles and variable flow rate. Mathematical Modelling in Civil Engineering* **14** (2), 13–25. <https://doi.org/10.2478/mmce-2018-0004>.
- Al-kizwini, R. S. 2015 Improvement of sedimentation process using inclined plates. *Mesopotamia Environmental Journal* **2** (1), 100–114.
- ANSYS, C. 2016 *ANSYS-CFX-Solver Theory Guide Release 17.2*. ANSYS Inc., Canonsburg, PA.
- Asgharzadeh, H., Firoozabadi, B. & Afshin, H. 2011 *Experimental investigation of effects of baffle configurations on the performance of a secondary sedimentation tank. Scientia Iranica* **18** (4), 938–949. <https://doi.org/10.1016/j.scient.2011.07.005>.
- Balwan, K., Mujawar, A., Bhabuje, D. & Karake, M. 2016 Study of the effect of length and inclination of tube settler on the effluent quality. *International Journal of Innovative Research in Advanced Engineering* **3**, 36–40.
- Carlsson, B. 1998 *An Introduction to Sedimentation Theory in Wastewater Treatment*. Systems and Control Group, Uppsala University, Uppsala, Sweden.
- Fadel, A. A. 1985 *Model for Horizontal Tube Settlers. Doctoral Dissertation*, Iowa State University, Iowa.
- Faraji, A., Asadollafardi, G. & Shevidi, A. 2013 A pilot study for the application of one- and two-stage tube settlers as a secondary clarifier for wastewater treatment. *International Journal of Civil Engineering* **2** (4), 272–280.
- Fouad, H. A., Elhefny, R. M. & Marei, A. I. 2016 *Evaluating the use of tube settlers and lamella plates in increasing the efficiency of sedimentation tanks. Journal of Applied Life Sciences International* **7** (4), 1–8. <https://doi.org/10.9734/JALSI/2016/28579>.
- Gao, H. 2019 *Computational Fluid Dynamics Modelling of Secondary Settling Tank. Doctoral Dissertation*, University of California, Los Angeles, USA.
- Gkesouli, A. 2018 *CFD Modeling of Wind Effect on the Hydrodynamic Behavior and Removal Efficiency of Settling Tanks. Doctoral Dissertation*, School of Civil Engineering, National Technical University of Athens, Athens, Greece.
- Gurjar, A., Bhorkar, M., Bhole, A. G. & Baitule, P. 2017 *Performance of tube settler module. International Journal of Engineering Research and Application* **7** (3), 52–55. <https://doi.org/10.9790/9622-0703065255>.
- Henricks, D. 2011 *Fundamentals of Water Treatment Unit Processes: Physical, Chemical and Biological*. CRC Press, Boca Raton, FL.
- Ishii, M. 1975 *Thermo-Fluid Dynamic Theory of Two-Phase Flow*. Collection de la Direction des Etudes et Researches de EDF, Eyrolles, 22, Paris, France.
- Nguyen, T., Dao, N. T., Liu, B., Terashima, M. & Yasui, H. 2019a *Computational fluid dynamics study on attainable flow rate in a lamella settler by increasing inclined plates. Journal of Water and Environment Technology* **17** (2), 76–88. <https://doi.org/10.2965/jwet.18-044>.
- Nguyen, T., Dao, N. T., Terashima, M. & Yasui, H. 2019b *Improvement of suspended solids removal efficiency in sedimentation tanks by increasing settling area using computational fluid dynamics. Journal of Water and Environment Technology* **17** (6), 420–431. <https://doi.org/10.2965/jwet.19-052>.

- Sharma, A. & Bhatia, R. K. 2018 Comparative study on effect of variation in diameter, inclination, length of tubes in tube settler module on the water quality. *International Journal for Research in Applied Science & Engineering Technology* **6** (10), 677–680.
- Stamou, A. & Gkesouli, A. 2015 [Modelling settling tanks for water treatment using computational fluid dynamics](#). *Journal of Hydroinformatics* **17** (5), 745–762. <https://doi.org/10.2166/hydro.2015.069>.
- Tamayol, A., Firoozabadi, B. & Ahmadi, G. 2008 [Effects of inlet position and baffle configuration on hydraulic performance of primary settling tanks](#). *Journal of Hydraulic Engineering* **134** (7), 1004–1009. [https://doi.org/10.1061/\(ASCE\)0733-9429\(2008\)134:7\(1004\)](https://doi.org/10.1061/(ASCE)0733-9429(2008)134:7(1004)).
- Tarpagkou, R. & Pantokratoras, A. 2014 [The influence of lamella settler in sedimentation tanks for portable water treatment-A computational fluid dynamic study](#). *Powder Technology* **268**, 139–149. <https://doi.org/10.1016/j.powtec.2014.08.030>.
- Yu, Y., Liu, D. & Cui, X. 2016 Study on hydraulic characteristics of the tube settler. In: *Proceedings of the 2016 International Conference on Mechatronics, Control and Automation Engineering*, 24–25 July 2016, Bangkok, Thailand. Atlantis Press, pp. 128–131. <https://doi.org/10.2991/mcae-16.2016.31>.

First received 7 October 2022; accepted in revised form 26 March 2023. Available online 11 April 2023